The effects of operating conditions and the biomass component on combustion efficiency and emission performance of a swirling fluidized-bed combustor fired using

Janya Udomsup, Prasan Choomjaihan*

(Department of Agricultural Engineering, Faculty of Engineering, King Mongkut's Institute of Technology Ladkrabang, Bangkok, 10520, Thailand)

Abstract: This work presents a study for biomass possible to bring renewable energy in a swirling fluidized bed combustor (SFBC). The main objective of this experimental work was to study the biomass component and excess air of biomass. Palmyra palm shell, Leucaena (lam.), and water hyacinth are using as fuel in the tests. Quartz sand of 600-850 μm and static bed height of 20 cm was used as inert bed material. For all of the tests, the feed rate was fixed as 45 kg h^{-1} for variable excess air (of 40%, 60% and 80%). As the experimental results, the temperature profiles in SFBC were obviously seen deviate when tests with higher excess air. In the test run, the highest cellulose (palmyra palm shell) for 80% excess air had CO and NO emissions were found in quite stable level (less than 250 and 300 ppm, respectively). The combustion efficiency more than 99% could be achieved in this work.

Keywords: biomass, biomass component, efficiency, emission, fluidized-bed, combustion, swirling

Citation: Udomsup, J., and P. Choomjaihan. 2021. The effects of operating conditions and the biomass component on combustion efficiency and emission performance of a swirling fluidized-bed combustor fired using. Agricultural Engineering International: CIGR Journal, 23(2): 195-202.

1 Introduction

Development of alternative renewable energy has been continuously improved in recent times because of the rapidly increasing of the use of energy which is leaded to the energy insecurity and environmental cum sociopolitical issues associated with the use of fossil fuels. Biomasses in term of agricultural resources supply energy in two forms from energy crops and their residue. Therefore, the fast-growing energy crops, biomasses, with less impact on environmental pollution has been intensively explored which hope of that they can be substituted with the current fossil energy source issue. Significant researches have been devoted to the production of activated carbons from agricultural waste materials and based on biomass main components (hemicellulose, cellulose and lignin). In this research, the tree biomasses represented the crop residue and fast-growing tree (both land crop and aquatic plant) were selected. Palmyra palm shell, Leucaena (lam.), and Water hyacinth were, then, used as the raw material throughout this research. Among the varieties of combustion technologies, fluidized-bed combustion has proven that it is suitable for burning alternative solid fuel, due to its highly efficiency in converting fuels to clean energy, fuel flexibility, clean operation and so on

Received date: 2019-08-13 **Accepted date:** 2020-02-10
***Corresponding author: Prasan Choomjaihan**, Department of Agricultural Engineering, Faculty of Engineering, King Mongkut's Institute of Technology Ladkrabang, Bangkok, Thailand. Tel: 023298337-8. Fax: 023298336. Email: prasan.ch@kmitl.ac.th.

(Natarajan et al.,1998; Anthony, 1995; Scala and Chirone, 2004; Armesto et al., 2002). Recently, two novel combustion techniques ensuring fuel oxidation in a strongly swirled flow have been developed and tested for burning biomass (Eiamsa-Ard et al., 2008; Madhiyanon et al., 2006). The swirled flow in the combustor is controlled by two sections a vortex combustor and a cyclonic fluidized-bed combustor which gives more than 99% of combustion efficiency and lower than 400 ppm of CO emission. In the combustor, a swirling fluidized-bed is generated by primary air introduced into the bed through an annular spiral air distributor, as rotational gas-solid flow in the combustor freeboard is sustained by secondary air injected tangentially into the bed splash zone. High combustion efficiency at rather low major emissions is ensured in this swirling fluidized-bed combustor firing rice husk over wide ranges of fuel properties and operating condition (Kuprianov et al., 2010).

Therefore, this work was aimed to study the combustion of Palmyra palm shell, Leucaena (lam.), and water hyacinth, of some biomass component, in the swirling fluidized-bed combustor using quartz sand as the bed material to prevent bed agglomeration. Effect of excess air (a key operating parameter of the combustor) on the behavior of major gaseous pollutants (CO and NO) in different regions inside the combustor was the focus of experimental tests.

2 Experimental

2.1 Experimental set-up

In the combustion tests, the mean particle size of biomasses and excess air were chosen as independent variable, whereas the fuel feed rate was maintained to be constant 45 kg h^{-1}, in all the combustion tests. The swirling fluidized bed combustor (SFBC) were carried out for three values of excess air of about 40%, 60%, and 80%.

Figure 1 depicts schematic diagram of experimental set-up of the SFBC. The combustor was made from 4.5 mm thick steel covered internally with 50 mm thick insulation fabricated from refractory cement. A combustor body consisted of two part, a conical section with a 40° cone angle, 1 m height and 0.25 m diameter at the bottom base, and a cylindrical section with 2.5 m height and 0.9 m inner diameter. An annular spiral distributor for the combustor was made up of stainless steel with the same geometrical characteristics as those of the swirl generator in the ‘cold’ model. Quartz sand with the size of 0.6 to 0.8 mm set at 20 cm static bed height were used as the inert bed material in the combustor. To stabilize the swirl motion of the gas-solid bed, a steel cone with 80-mm diameters at its lower base was set at the top of the air distributor, as shown in Figure1 A screw-type feeder delivered biomass over the bed at a 0.6 m level above the air distributor, which a 25 hp blower supplied primary air (at ambient condition) into the combustor through the distributor. An external cyclone at the top of the SFBC served for separation of particulate matters (char, ash and carryover sand particles) from the flue gas leaving the combustor.

The concentrations of gaseous pollutants (CO and NO) in flue gas were measured in the experimental tests along the height of combustor above the air distributor when firing the selected biomass fuels. In addition, concentrations as well as temperatures were detected along the combustor height and in the flue gas at the cyclone outlet (see Figure 1). For each test run, the value of excess air in the flue gas was determined using the O_2 and CO concentrations at the cyclone outlet. The Testo-350XL gas analyzer was employed for measuring the gas concentrations (CO, NO, and O_2) and temperature. They were measured along axial directions in the conical SFBC, as well as at the exit of an ash-collecting cyclone downstream from the combustor. The relative measurement errors were of 0.5% for the temperature, 5% for CO ranged from 100-2000 ppm, 10% for higher than 2000 ppm, 5% for NO and 0.2% for O_2. Chromel-alumel thermocouples were set at difference levels along the combustor height and at the cyclone outlet to monitor the temperatures (in relative error of about 1%) in the flue gas.

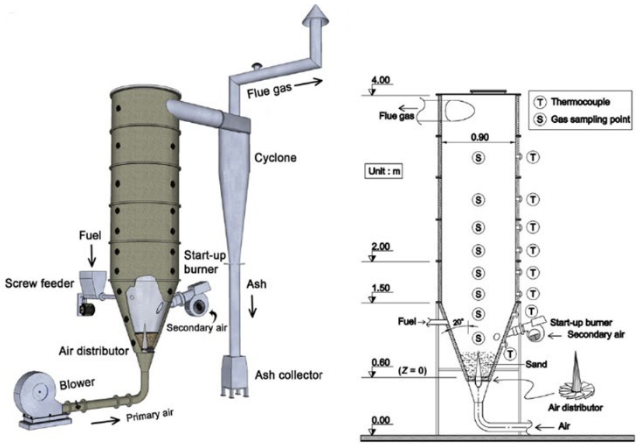

Figure 1 Schematics of the experimental set-up with a laboratory-scale conical SFBC (Kaewklum et al., 2010)

2.2 Fuel ultimate analysis and heating value

The results of the ultimate, proximate analyses and the low heating value (LHV) were provided in Table 1. It was illustrated in Table 1 that the biomass included a significant amount of volatile matter, whereas fuel moisture and ash were at quite low level, which resulted in a substantial heating value of the biomass.

Table 1 The ultimate, proximate analyses and the LHV of biomasses

Biomass	Ultimate analysis (wt.%, on "as-received" basis)					Proximate analysis (wt.%, on "as-received" basis)				
	C	H	O	N	S	W	A	VM	FC	LHV (kJ kg^{-1})
Leucaena (lam.)	44.18	6.37	42.25	2.01	0.26	12.15	4.65	71.49	11.70	15,570
Palmyra Palm shell	47.14	6.26	44.42	0.20	0.08	9.65	1.82	71.65	16.80	16,630
Water hyacinth	27.79	4.55	34.39	0.93	0.32	9.24	31.02	57.31	2.42	9,670

Note: W=fuel moisture; A=fuel ash; VM=volatile matter; FC= fixed carbon

2.3 Method for thermogravimetric/derivative thermogravimetric analysis of biomass

The ground samples left from higher heating value determination were subjected for thermogravimetric analysis. The combustion characteristic of biomasses was performed in the thermogravimetric analyzer. At the heating rate of 10°C min^{-1}, the temperature of furnace was increased from 30°C to 1000°C in an air flux (O_2) of 20 mL min^{-1}.

3 Results and discussion

3.1 Biomass compositions

The hemicellulose, cellulose and lignin weight fractions present within those natures lignocellulosic materials have been also determined following procedure described in detail elsewhere (Saeman et al., 1954). As shown in Figure 2, the raw materials presented very different compositions. The highest holocellulose (the cellulose combined with hemicellulose) is was Palmyra Palm shell. For the biomass that has the most lignin content is water hyacinth, Palmyra Palm shell and Leucaena (lam.), respectively. The total composition (the hemicellulose, cellulose and lignin) of the biomass of Palmyra Palm shell is the highest. The low heating value of Palmyra Palm shell will be high as well.

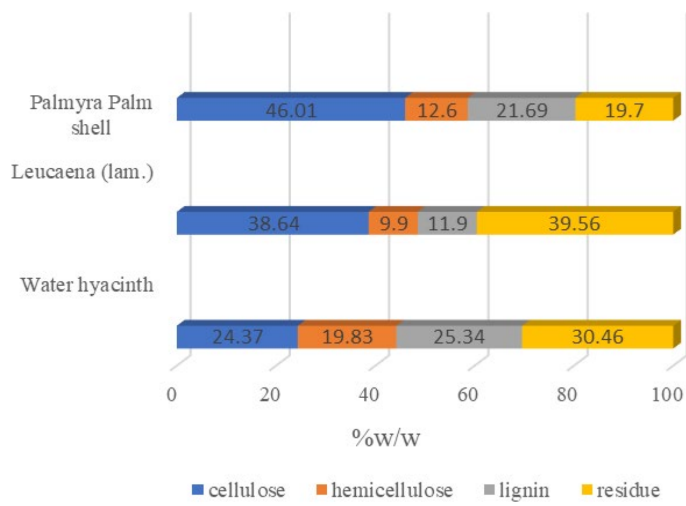

Figure 2 Composition of biomasses: cellulose, hemicellulose, lignin and residue

3.2 Thermogravimetric characteristics of biomasses

Thermogravimetric (TG) analyzer was employed to obtain TG and derivative thermogravimetric (DTG) curves of biomass (Leucaena (lam.), Palmyra palm shell, water hyacinth) for the characteristics of them. During each TG test, sample were heated from 30°C to 900°C at a constant heating rate of 20°C min^{-1}, typical for a TG analysis of various biomasses (Kuprianov and Arromdee, 2013; Ninduangdee and Kuprianov, 2014). Figure 3 illustrated that the thermal decomposition of biomass has four ranges. The first phase, the removal of moisture in the biomass material, was set the temperature between 30°C-200°C. Phase 2: The temperature between 220°C-300°C was for the decomposition of hemicellulose structure. Phase 3: The temperature between 300°C-340°C was for the decomposition of cellulose structure. Finally, the temperature over 340°C was for the decomposition of lignin structure.

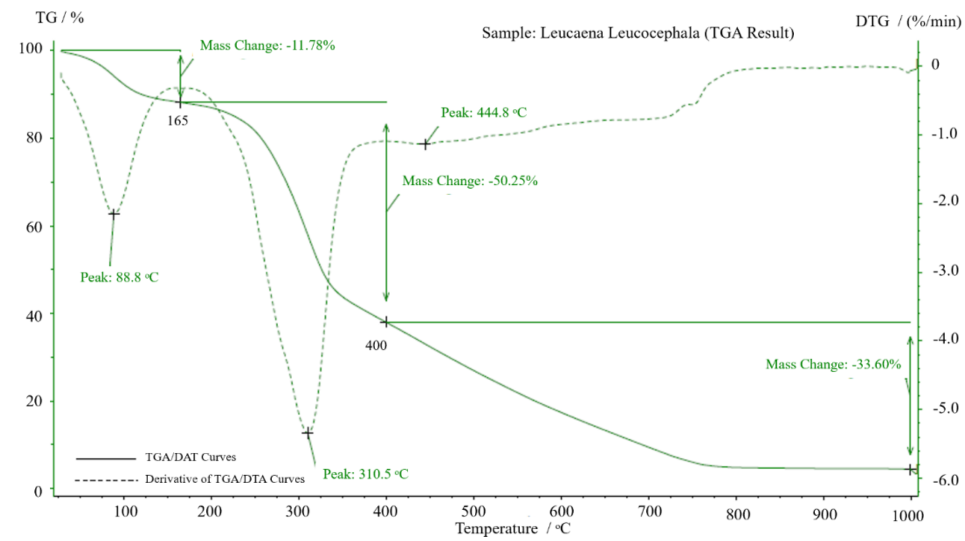

(a)

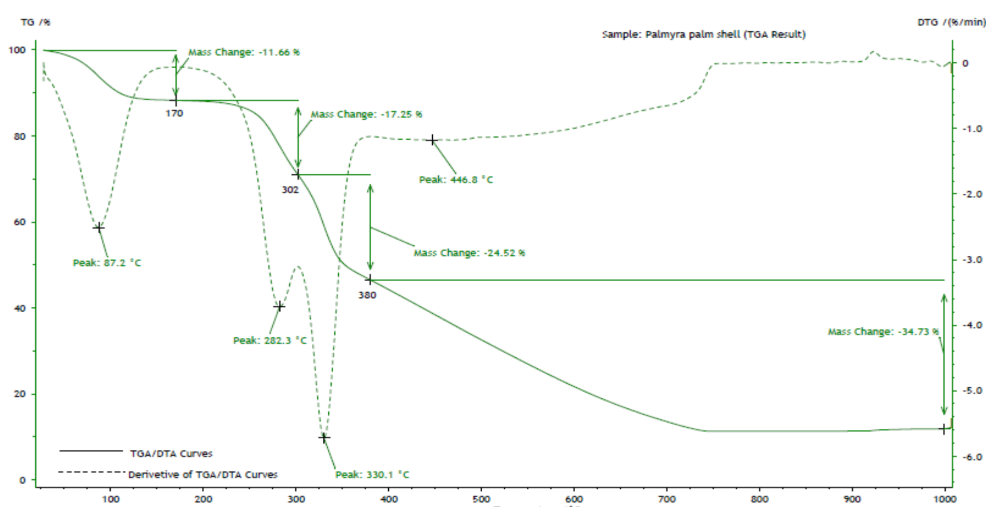

(b)

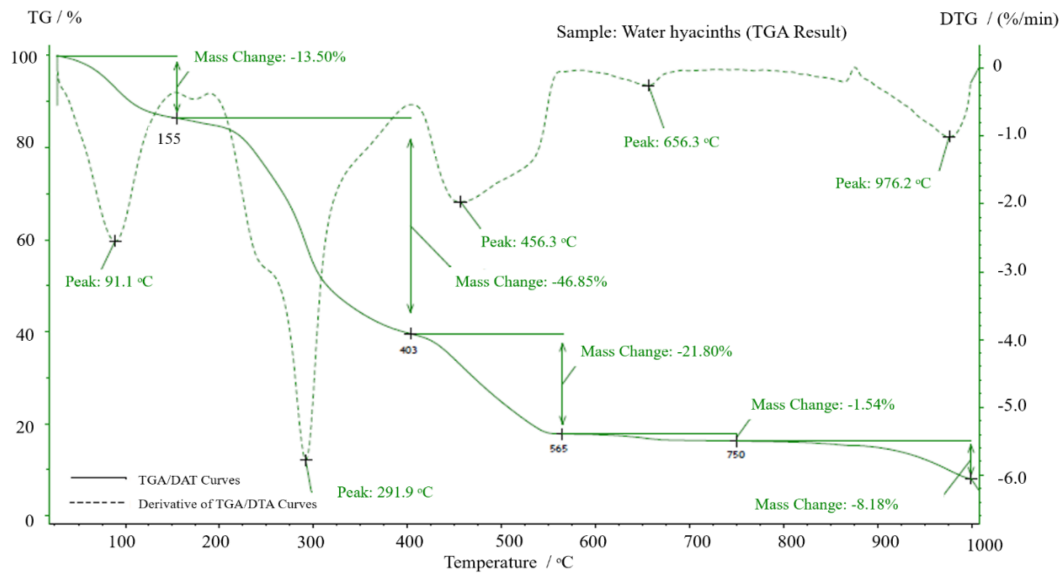

(c)

Figure 3 TG/DTA profile of biomass (a) is Leucaena (lam.), (b) is Palmyra palm shell, (c) is water hyacinth

3.3 Emission profiles in the SFBC

Figure 4 shows the effects of excess air (40%, 60%, and 80%) and biomass components on the axial CO and NO concentration profiles. In all the test runs, the axial CO concentration profile were found to have a maximum, CO_{max}, at a certain location above the air distributor (at Z=0.6 m). The rate of CO formation for the high biomass components (Palmyra Palm Shell) was higher than water hyacinth and Leucaena (lam.), which resulted in difference CO_{max} values for these fuels. CO exhibited a tremendous increase (axial gradient) along the combustor height, mainly caused by the holocellulose (the cellulose combined with hemicellulose) (Cagnon et al., 2009). The apparent difference in the axial CO concentration profiles for difference biomass components confirms a significant role of heterogeneous reaction (on the char surface) of char-carbon with CO_2 and water vapor (Cagnon et al., 2003). These reactions basically follow the fuel “in-bed devolatilization” (Z≤0.6 m) and further oxidation of the carbonaceous components (released from the fuel particles with volatiles) to CO (Werther et al., 2000; Turn, 2006). In the reduction region, the CO was basically oxidized in the reaction with OH radicals as well as by oxygen directly (Tillman et al., 1981). The rates of CO reduction in the freeboard region were in apparent correlation with CO concentration, as confirmed by the profiles in Figure 4a.

Simultaneously, significant reduction in the CO concentration along the combustor height occurred in the freeboard region, where CO was likely oxidized in homogeneous with OH radicals and O_2. For the fuel option, CO concentrations at all the locations of the combustor were lowered with higher excess air values. However, the effects of excess air on the CO concentrations were found to be rather strong for relatively low excess air values (40%), whereas they were almost negligible for excess air = 80%.

In NO measurement, NO concentration in the flue gas at different combustor locations did not exceed 1 ppm. That was why the NO in the discussion below was represented by NO only. Figure 4b compares the axial NO concentration profiles in the SFBC for the same, as in Figure 4a, fuel options and operating conditions. Like CO, all the axial NO concentration profiles possessed a maximum, NO_{max}, where location made it possible to distinguish conventionally the formation and reduction regions for this pollutant.

As shown in Figure 4b, the rates of both NO formation (in the bed region) and NO reduction (in the freeboard region) for firing Leucaena (lam.) were found to be higher than those for Palmyra palm shell and water hyacinth. This difference in the NO formation was apparently correlated to the fuel-N content, while the NO reduction was affected by the ash, catalytic reaction of NO with CO on the surface of char.

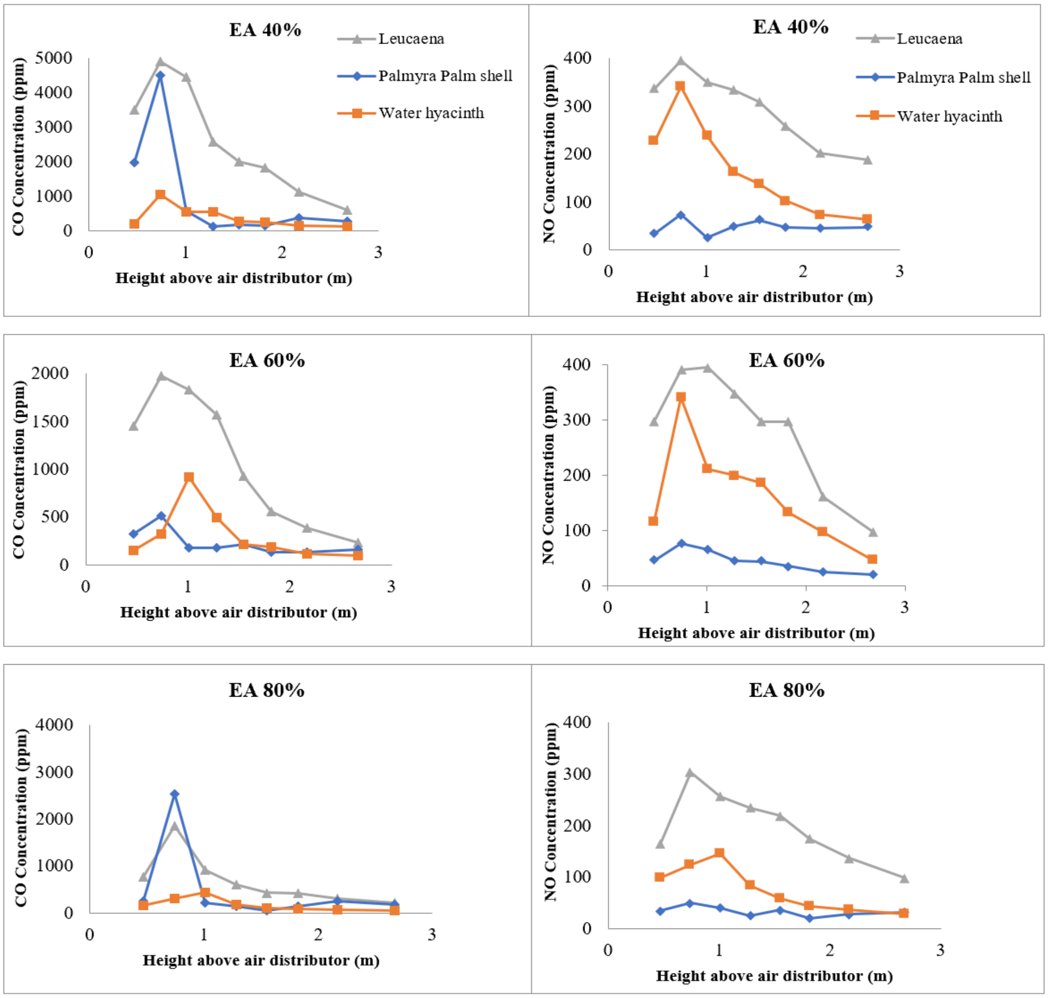

(a) (b)

Figure 4 Effects of excess air and biomass component (a) the axial CO concentration profile and (b) the axial NO concentration profile in SFBC.

3.4 Combustion efficiency

Table 2 compares the heat losses with unburned carbon and owing to incomplete combustion as well as the combustion efficiencies of the SFBC for firing biomasses. Within the range of applied operating conditions (excess air), the decreasing in the cellulose content led to deterioration of the combustion efficiency, accompanied, however, by the reduction in NO emissions from the combustor. The reduction in the combustion efficiency could be explained by the noticeably increase in the heat loss with unburned carbon, while the heat loss owing to incomplete with unburned carbon was weakly affected by cellulose content.

As may be generally concluded, the best performance of the SFBC could be achieved at different values of excess air: while high cellulose content could be burned at excess air =40%-60%, the combustion of biomass of deteriorated quality (low cellulose content) requires higher values of excess air, excess air =80%.

Table 2 Heat losses and combustion efficiency for the SFBC firing biomasses with different component and different value of excess air.

Cellulose content	Biomass	Excess air (%)	Heat loss with unburned carbon (%)	Heat loss owing to incomplete with unburned carbon (%)	Combustion efficiency (%)
46	Palmyra palm shell	40	0.039	0.101	99.86
		60	0.035	0.074	99.89
		80	0.03	0.092	99.89
39	Leucaena (lam.)	40	0.425	0.173	99.4
		60	0.367	0.109	99.52
		80	0.347	0.042	99.61
24	Water hyacinth	40	6.352	0.067	93.58
		60	15.274	0.054	84.67
		80	3.601	0.043	96.36

4 Conclusions

The SFBC has been successfully tested for firing 45 kg h^{-1}, the biomass with variable cellulose content, from 20% to 50%, at different percentages of excess air (of about 40%, 60% and 80%).

During the experimental tests, data on CO and NO concentrations along the combustor height were generated for the above fuel qualities and operating conditions.

The following major conclusions have been derived from this work:

(1) The biomass component and excess air have important effects on formation of pollutions at the SFBC bottom and their oxidation (for CO) or reduction (for NO) in freeboard, and consequently, on the combustion efficiency and emissions of the SFBC. The emission of CO can be effectively mitigated by decreasing the biomass composition and/or increasing excess air, whereas the NO emission can be reduced by increasing the biomass component and/or via lowering the amount excess air. Thus, both biomass component and excess air have sensible effects on the formation/reduction of CO and NO in the bottom/freeboard regions of the combustor.

(2) The temperature profiles in SFBC were obviously seen deviate when tests with higher excess air. In the test run, the highest cellulose (Palmyra Palm Shell) for 80% excess air had CO and NO emissions were found in quite stable level (less than 250 and 300 ppm, respectively). The combustion efficiency more than 99% could be achieved in this work.

From optimal conditions, the biomass, which is highest cellulose (Palmyra Palm Shell) could be operated with high (99%) combustion efficiency ensuring the minimum emission (or "external") costs of the proposed combustion biomass for SFBC.

Acknowledgments

The authors wish to acknowledge sincerely the financial support from Faculty of Engineering, King Mongkut's Institute of Technology Ladkrabang (KMITL), Thailand.

References

Anthony, E. J. 1995. Fluidized bed combustion of alternative solid fuels: status, success and problems of technology. *Progress in Energy and Combustion Science*, 21(3): 239-268.

Armesto, L., A. Bahillo, K. Veijonen, A. Cabanillas, and J. Otero. 2002. Combustion behavior of rice husk in a bubbling fluidized bed. *Biomass and Bioenergy*, 23(3): 171-179.

Cagnon, B., X. Py, A. Guillot, and F. Stoeckli. 2003. The effect of carbonization/activation procedure on the microporous texture of the subsequent chars and active carbons. *Microporous and Mesoporous Materials*, 57(3): 273-282.

Cagnon, B., X. Py, A. Guillot, F. Stoeckli, and G. Chambat. 2009. Contributions of hemicellulose, cellulose and lignin to the mass and the porous properties of chars and steam activated carbons from various lignocellulosic precursors. *Bioresource Technology*, 100(1): 292-298.

Eiamsa-Ard, S., Y. Kaewkohkiat, C. Thianpong, and P. Promvonge. 2008. Combustion behavior in a dual-staging vortex rice husk combustor with snail entry. *International Communications in Heat Mass Transfer*, 35(9): 1134-1140.

Kaewklum, R. and Kuprianov, I. V. 2010. Experimental studies on a novel swirling fluidized-bed combustor using an annular spiral air distributor. Fuel 89(1), 43–52.

Kuprianov, V. I., and P. Arromdee. 2013. Combustion of peanut and tamarind shells in a conical fluidized-bed combustor: a comparative study. *Bioresource Technology*, 140: 199-210.

Kuprianov, V. I., R. Kaewklum, K. Sirisomboon, P. Arromdee, and S. Chakritthakul. 2010. Combustion and emission characteristics of a swirling fluidized-bed combustor burning moisturized rice husk. *Applied Energy*, 87(9): 2899-2906.

Madhiyanon, T., A. Lapirattanakun, P. Sathitruangsuk, and S. Soponronnarit. 2006. A novel cyclonic fluidized-bed combustor (ψ-FBC): Combustion of thermal efficiency, temperature distribution, combustion intensity, and emission of pollutants. *Combustion and Flame*, 146(1-2): 232-245.

Natarajan, E., A. Nordin, and A. N. Rao. 1998. Overview of combustion and gasification of rice husk in fluidized bed reactors. *Biomass and Bioenergy*, 14(5-6): 533-546.

Ninduangdee, P., and V. I. Kuprianov. 2014. Combustion of palm kernel shell in a fluidized bed: Optimization of biomass particle size and operating conditions. *Energy Conversion and Management*, 85: 800-808.

Saeman, J. F., W. E. Moore, R. L. Mitchell, and M. A. Millett. 1954. Techniques for the determination of pulp constituents by quantitative paper chromatography. *Tappi Journal*, 37(8): 336-343.

Scala, F., and R. Chirone. 2004. Fluidized bed combustion of alternative solid fuels. *Experimental Thermal and Fluid Science*, 28(7): 691-699.

Tillman, D. A., A. J. Rossi, and W. D. Kitto. 1981. *Wood Combustion: Princples, Processes, and Economics*. New York: Academic Press.

Turn, S. R. 2006. *An Introduction to Combustion*. 2nd ed. Boston: McGraw-Hill.

Werther, J., M. Saenger, E. U. Hartge, T. Ogada, and Z. Siagi. 2000. Combustion of agricultural residues. *Progress in Energy and Combustion Science*, 26(1): 1-27.